Available online at www.sciencedirect.com
SCIENCE DIRECT®
Composites: Part A 34 (2003) 1265–1271
composites
Part A: applied science and manufacturing
www.elsevier.com/locate/compositesa

Four-point bend interlaminar shear testing of uni- and multi-directional carbon/epoxy composite systems

P. Feraboli*, K.T. Kedward

Department of Mechanical and Environmental Engineering, University of California, Santa Barbara, CA 93106, USA

Accepted 6 February 2003

Abstract

Purpose of the paper is to investigate the possibility of extending the interlaminar shear strength (ILSS) results obtained by four-point bend testing of unidirectional laminates to multidirectional laminates, such as cross-ply and quasi-isotropic, the testing of which is a common practice in the industry but has not been previously validated in the literature. An experimental database is gathered through the known modified version of the ASTM D2344 short beam test and the results show a surprising proximity of results for the three different fiber architectures for the same composite system. Various finite element analyses were developed using ANSYS® software, allowing for better insight on the mechanics of delamination in four-point bending, and showed extremely good agreement with the experimental values. The final and most accurate model partially confirmed observations made by other authors, and includes the 'skewed' profile of the shear stress through the thickness and its variation along the length, the distribution of the shear stress across the width, the location of delamination initiation and propagation and maximum ILSS and the shear stress contour.

Keywords: Four-point bend; Short beam shear test; Interlaminar shear; Delamination; Carbon/epoxy

1. Introduction

The highly anisotropic nature of laminated composite structures causes a mismatch in mechanical properties between individual laminae within the laminate, which in turn can produce delamination initiation and propagation. Interlaminar shear stress develops at the free edge of multidirectional laminates and at local discontinuities such as notches, ply-drops, bonded and bolted joints, where ply stresses must become zero to satisfy boundary conditions. According to current yet not extensive literature, these stresses need to be evaluated for structural applications and many authors feel that delamination growth is the fundamental issue in the evaluation of laminated composite systems for durability and damage tolerance.

Three-point bending test, also known as short beam shear test, is often used to measure the apparent interlaminar shear strength (ILSS) of composite laminates. Since concerns arise about this test because of the strong localized damage occurring underneath the loading roller, a modified version of the test, the four-point bending test, is more frequently used, as in the present work, because of its better distribution of the load. Previous experimental and analytical work [3,8,11] on unidirectional carbon–epoxy showed that changing the support span over thickness (s/t) ratio has dramatic effects on the measured short beam and four-point bend shear strengths. The actual stress-state in a given beam specimen is three-dimensional, with stresses varying through the thickness and along the length and therefore cannot be adequately interpreted by means of classical beam theory. Early theoretical work [4] also predicted a variation of shear stresses across the width, with peaks at the edge of the coupon. Experimental work [5] by means of Moiré fringe interferometry showed an interesting discontinuous distribution of the shear strain through the thickness of the specimen, with peaks at the ply interfaces where compliant resin-rich regions are formed and delamination tends to originate. The present work intends to verify some of these previously reported results for unidirectional laminates and investigate their applicability

* Corresponding author. Tel.: +1-805-893-3381; fax: +1-805-407-1123.
E-mail addresses: pmc@engineering.ucsb.edu (P. Feraboli), kedward@engineering.ucsb.edu (K.T. Kedward).

1359-835X/03/$ - see front matter © 2003 Elsevier Ltd. All rights reserved.
doi:10.1016/S1359-835X(03)00204-5

to more complex fiber architectures and stacking sequences.

2. Experimental

2.1. Specimens: preparation and characteristics. Test procedure: fixture and parameters

The laminates tested were unidirectional $[0°]_s$, cross-ply $[0/90°]_s$ and quasi-isotropic $[0/\pm 45/90°]_s$ lay-ups of carbon fiber reinforced epoxy impregnated tape. From the laminates a total of 30 coupons were cut with a diamond coated tip table saw, in the longitudinal direction. Strips of material approximately 1/4 in. (6.35 mm) in width were cut at the plate boundary in order to avoid any external influences on the testing procedure, such as long-time environmental exposure, possible impacted material and manufacturing related boundary defects. The average geometry was 1.300 in. (33 mm) length, 0.300 in. (7.6 mm) width, 0.165 in. (4.2 mm) thickness and the standard deviation in the measured dimensions was negligible. Therefore, an *s*/*t* ratio of 8.0 is used, twice the ratio prescribed by ASTM D2344 [1] for three-point bend, in order to give the same nominal stress in the central region (Fig. 1).

The coupons were placed in a sliding roller four-point bending fixture (Fig. 2) with an inner and outer span of 0.5 and 1.25 in. (12.7 and 31.7 mm), respectively. The samples were tested to failure (Mean static failure load MSFL) on an Instron 1123 electro-mechanical, double-screw test frame under displacement control. Other test Settings were crosshead feed rate of 0.02 in./min (0.5 mm/min) and 2 Hz sampling rate on IBM PC-type computer. The flexural strength of the material was also measured using the same general-purpose fixture by simply adjusting the inner and outer spans and by using a specimen geometry conforming to ASTM D790 [6] specifications.

2.2. Results and discussion

2.2.1. Interlaminar shear testing

Failure occurs suddenly in a macroscopically brittle mode by crack initiation and propagation. A single crack propagates from a region located about one thickness away

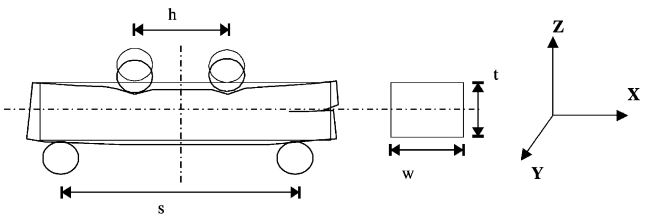

Fig. 1. Deformed and non-deformed configurations of ILS specimen.

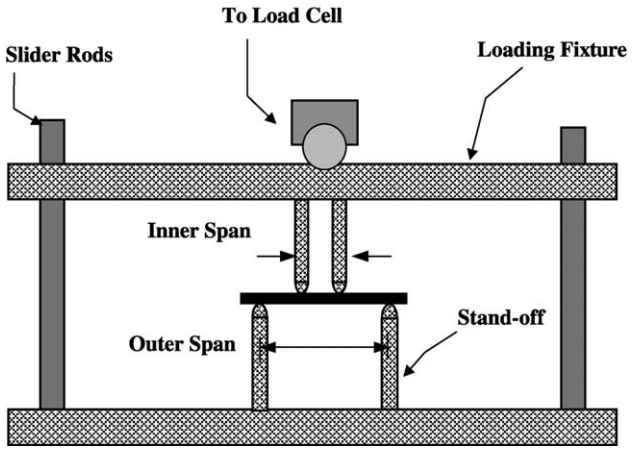

Fig. 2. Four-point bend fixture and specimen.

from the support, usually at the axis of symmetry or within a 1/4 of the thickness above. A sharp drop in the load–displacement curves and an audible cracking sound accompany catastrophic delamination. After the first inter-ply failure, which in the present work is used for calculating the ILSS, load picks up again and in some cases the peak load may reach the original value. In few tests failure was not visible at the time of the load drop, but upon removing the specimen or with slightly higher displacement it would manifest visibly.

The interlaminar shear stress results are reported in Tables 1–3 for each coupon and laminate architecture.

The simple beam theory yields the expression for the max shear stress in a

$$\tau = \frac{3}{4}\frac{P}{wt} \tag{1}$$

homogeneous beam.

Concerns were previously expressed [2,3,7,12] on the variability of the ILS strength with the degree of orthotropy of the material. As summarized in Table 5, it is possible to assert that the results obtainable from testing unidirectional specimens can be used to assess the behavior of more complex configurations of the same geometry and composite system. This discussion is directed only to a comparison based on first inter-ply failure, which is the commonly accepted indication of failure for this type of test. However, the structure can continue to sustain considerable loads way beyond fracture initiation, particularly for laminates with multiple fiber orientation. Further work should be done in the fracture propagation regime and a comparison of results between uni- and multi-directional specimens up to ultimate load might reveal substantial discrepancies.

2.2.2. Flexural testing

According to ASTM standard D790, the same four-point bend fixture was used, with a geometry of $4 \times 1 \times 0.165$ in.^{3} ($101.6 \times 25.4 \times 4.2$ mm^3) and inner and outer spans of 1.5 and 3.75 in. (38.1 and 95.2 mm), respectively to determine

Table 1
Unidirectional test results

Specimen	Thickness in. (m)	Width in. (m)	Length in. (m)	Load lb ft (N)	ILSS psi (MPa)
Uni 1	0.136 (0.0035)	0.254 (0.0065)	1.330 (0.0338)	511 (2273)	11095 (76.5)
Uni 2	0.140 (0.0036)	0.247 (0.0063)	1.347 (0.0342)	495 (2201)	10736 (74.0)
Uni 3	0.139 (0.0035)	0.239 (0.0061)	1.350 (0.0343)	499 (2219)	11265 (77.7)
Uni 4	0.139 (0.0035)	0.230 (0.0058)	1.351 (0.0343)	466 (2073)	10932 (75.4)
Uni 5	0.138 (0.0035)	0.222 (0.0056)	1.348 (0.0342)	472 (2100)	11555 (79.7)
Uni 6	0.139 (0.0035)	0.216 (0.0055)	1.354 (0.0344)	443 (1971)	11066 (76.3)
Uni 7	0.136 (0.0035)	0.237 (0.0060)	1.350 (0.0343)	479 (2131)	11146 (76.8)
Uni 8	0.141 (0.0036)	0.235 (0.0060)	1.348 (0.0342)	495 (2202)	11204 (77.2)
Uni 9	0.140 (0.0036)	0.238 (0.0060)	1.351 (0.0343)	490 (2180)	11029 (76.0)
Uni 10	0.142 (0.0036)	0.239 (0.0061)	1.350 (0.0343)	499 (2220)	11027 (76.0)
Avg.	0.139 (0.0035)	0.236 (0.0060)	1.348 (0.0342)	485 (2157)	11106 (76.6)
Sdev.	0.001 (0.00003)	0.015 (0.0004)	0.009 (0.0002)	20 (89)	216 (1.5)

the average flexural strength for the same laminates. The average values recorded for the unidirectional, cross-ply and quasi-isotropic laminates are, respectively, 179.15, 123.80, 129.67 ksi (1235, 853, 894 MPa). Failure manifests as fiber breakage and laminate splitting at the outer plies and the recorded values of the flexural strength are an order of magnitude greater than the interlaminar shear ones. So, while the flexural strengths of the three different architectures are substantially different due to their intrinsic fiber-dominated behavior, laminate stacking sequence does not affect the ILS strength because of its matrix-dominated nature, for the tested configuration and ply thickness, as much as other factors do, i.e. fiber volume, void content [11] and curing process parameters.

3. Analytical

3.1. Finite element model

The model used to reproduce the four-point bend coupon had dimensions based on the recorded average of the tested specimens. Only 1/4 of the coupon was analyzed, due to symmetry conditions. The laminates were modeled with 45 plies, each 0.0035 in. (0.09 mm) thick, and one element per ply was used throughout the entire study. A three-dimensional model was necessary to investigate through thickness and across width profiles of the ILS stress. Once a sound understanding of the behavior of the unidirectional laminate was gained, the cross-ply and the more complicated stacking sequence of the quasi-isotropic were investigated. For reference, it is reported that some early models were attempted with the aid of ANSYS element type Solid Quad 8 node 82 and Shell Linear layer 99, but they did not yield reliable ILS results or stress profiles. A better overall result was obtained with the Solid Layered 46 element, which allowed for fiber orientation in the case of the multidirectional laminates as well as ply interface and shear stress profile investigation. The total number of elements used in the final model was 9450 (Fig. 3). The applied load was half of the tested average MSFL 650 lb (2891 N) and it was prescribed as concentrated load (nodal force). The elastic properties of the baseline unidirectional tape are reported in Table 4.

Table 2
Quasi-isotropic test results

Specimen	Thickness in. (m)	Width in. (m)	Length in. (m)	Load lb ft (N)	ILSS psi (MPa)
Quasi 1	0.171 (0.0043)	0.255 (0.0065)	1.297 (0.0329)	652 (2900)	11236 (77.5)
Quasi 2	0.166 (0.0042)	0.271 (0.0069)	1.304 (0.0331)	648 (2882)	10803 (74.5)
Quasi 3	0.157 (0.0040)	0.267 (0.0068)	1.300 (0.0330)	624 (2776)	11164 (77.0)
Quasi 4	0.168 (0.0043)	0.283 (0.0072)	1.302 (0.0331)	744 (3309)	11736 (80.9)
Quasi 5	0.173 (0.0044)	0.298 (0.0076)	1.294 (0.0329)	772 (3434)	11231 (77.4)
Quasi 6	0.167 (0.0042)	0.298 (0.0076)	1.304 (0.0331)	728 (3238)	10971 (75.6)
Quasi 7	0.168 (0.0043)	0.282 (0.0072)	1.300 (0.0330)	692 (3078)	10955 (75.5)
Quasi 8	0.173 (0.0044)	0.271 (0.0069)	1.298 (0.0330)	684 (3043)	10942 (75.4)
Quasi 9	0.166 (0.0042)	0.273 (0.0069)	1.297 (0.0329)	678 (3016)	11221 (77.4)
Quasi 10	0.170 (0.0043)	0.301 (0.0076)	1.297 (0.0329)	772 (3434)	11158 (76.9)
Avg.	0.168 (0.0043)	0.280 (0.0071)	1.299 (0.0330)	699 (3109)	11158 (76.9)
Sdev.	0.005 (0.00013)	0.015 (0.0004)	0.003 (0.0001)	52 (231)	263 (1.8)

Table 3
Cross-ply test results

Specimen	Thickness in. (m)	Width in. (m)	Length in. (m)	Load lb ft (N)	ILSS psi (MPa)
Cross 1	0.165 (0.0042)	0.306 (0.0078)	1.304 (0.0331)	718 (3194)	10665 (73.5)
Cross 2	0.166 (0.0042)	0.302 (0.0077)	1.301 (0.0330)	738 (3283)	11041 (76.1)
Cross 3	0.165 (0.0042)	0.304 (0.0077)	1.298 (0.0330)	744 (3309)	11124 (76.7)
Cross 4	0.166 (0.0042)	0.253 (0.0064)	1.294 (0.0329)	620 (2758)	11072 (76.3)
Cross 5	0.161 (0.0041)	0.283 (0.0072)	1.302 (0.0331)	680 (3025)	11193 (77.2)
Cross 6	0.162 (0.0041)	0.291 (0.0074)	1.299 (0.0330)	700 (3114)	11137 (76.8)
Cross 7	0.163 (0.0041)	0.280 (0.0071)	1.297 (0.0329)	708 (3149)	11635 (80.2)
Cross 8	0.161 (0.0041)	0.244 (0.0062)	1.300 (0.0330)	580 (2580)	11073 (76.3)
Cross 9	0.159 (0.0040)	0.276 (0.0070)	1.297 (0.0329)	624 (2776)	10664 (73.5)
Cross 10	0.161 (0.0041)	0.302 (0.0077)	1.295 (0.0329)	738 (3283)	11384 (78.5)
Avg.	0.163 (0.0041)	0.284 (0.0072)	1.299 (0.0330)	685 (3047)	11099 (76.5)
Sdev.	0.002 (0.00005)	0.022 (0.0006)	0.003 (0.0001)	58 (258)	291 (2.0)

3.2. Results and discussion

From the finite element model, it was possible to plot the interlaminar shear stress contours (Figs. 5(1–3) that are very similar to the ones obtained in Ref. [3]. Nonetheless, the maximum and minimum values refer to the local stress concentration produced by the loading and supporting rollers, hence they are not representative of the strength of the laminates. By highlighting the central portion of the beam (Figs. 6(1–3) a more accurate distribution of the shear stress can be obtained. The peak occurs at about 1 thickness away from the support, at the symmetry axis or within a 1/4 of the thickness away, and its value confirms the test data for all three architectures (Table 5). This is suspected to be the location at which delamination originates. The values obtained by applying the prescribed average load (load-control approach) were also confirmed by running the model under a prescribed average displacement (displacement-control approach).

Investigation of the shear stress profile through the thickness at three different locations along the length Figs. 7(1–3) again confirmed the results obtained for unidirectional specimens in Ref. [3]. The concentration at the rollers is very high but rapidly decreases to values below the failure threshold in less than 1/12 of the thickness. It can be noted that in section b, away from the rollers, the profile is very similar to the one predicted by simple beam theory.

In Ref. [4], a close form elasticity solution was given to predict the three-dimensional variation of the shear stress across the width and the maximum value that would be reached at the lateral free edge. The results obtained are reported in Table 5; the model confirmed those predictions and the results are plotted in Figs. 8(1–3). In this case, the variation is contained within a few percent because of the small width of the specimen. It is noteworthy that the cross-ply yielded in both the calculation and FEA a much lower variation.

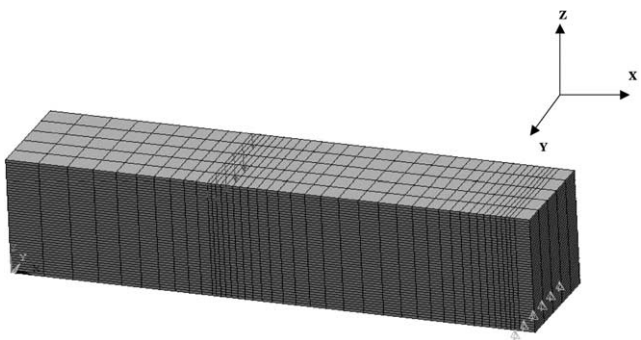

Fig. 3. In the depicted quarter portion of the ILS specimen, mesh, boundary conditions and load of final FEA model are highlited.

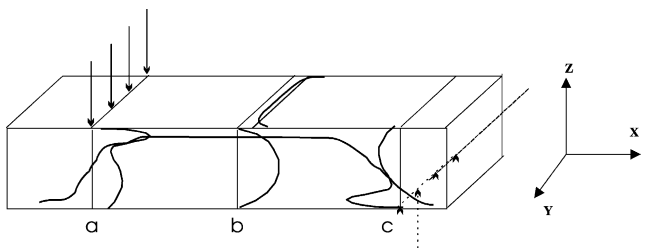

Fig. 4. Qualitative representation of the portion of the ILS specimen used in the FEA model; a, b, c represent the locations of interest for the stress profiles. The highlighted curves symbolize the distributions of the ILSS along the length, across the width and through the thickness and are reported in the following figures.

Table 4
Elastic properties for the unidirectional tape

$E_x = 18$ Msi (124.1 GPa)	$E_y = 1.5$ Msi (10.3 GPa)	$E_z = 1.5$ Msi (10.3 GPa)
$G_{xy} = 0.8$ Msi (55.2 GPa)	$G_{xz} = 0.8$ Msi (55.2 GPa)	$G_{yz} = 0.6$ Msi (4.1 GPa)
$\nu_{xy} = 0.3$	$\nu_{xz} = 0.3$	$\nu_{yz} = 0.35$

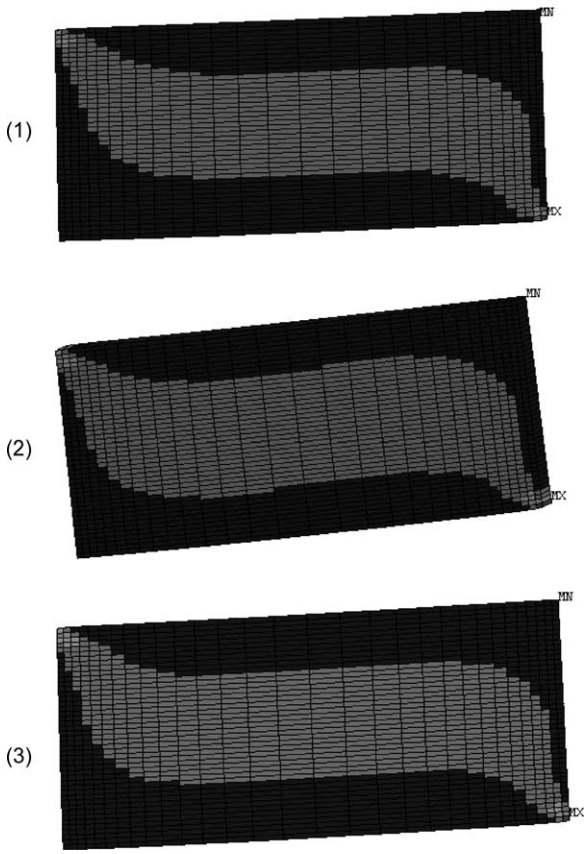

Fig. 5. 1/4 Model of ILS coupon: shear stress contour. (1) Unidirectional (2) Quasi-isotropic (3) Cross-ply.

The distribution of the shear stress along the length of the beam is depicted in Figs. 9(1–3). Theoretically, the beam should be subjected to constant shear loading and linearly increasing moment between the supporting and loading

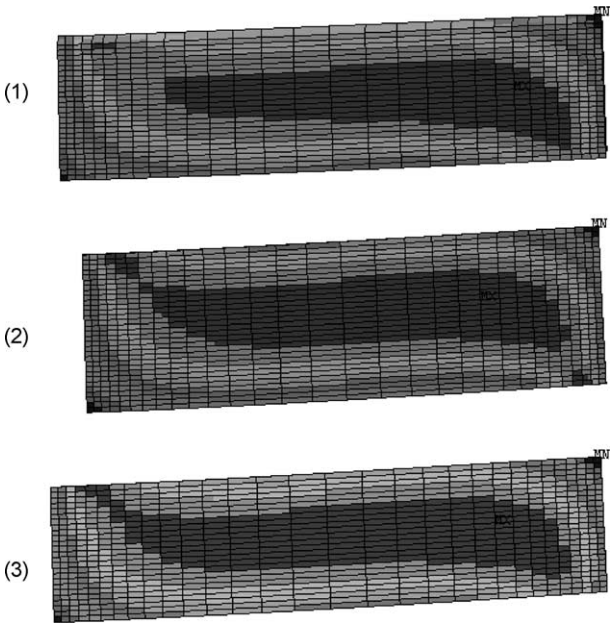

Fig. 6. 1/4 Model of ILS coupon: shear stress contour detail of critical area. (1) Unidirectional (2) Quasi-isotropic (3) Cross-ply.

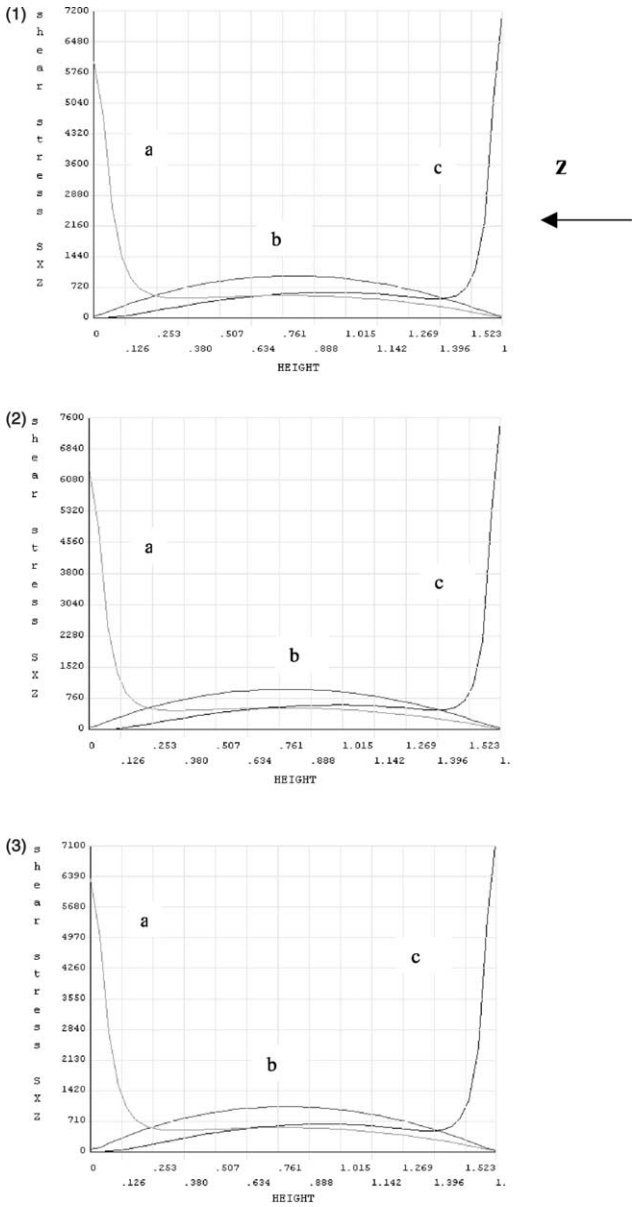

Fig. 7. 1/4 Model of ILS coupon: shear stress distribution through the thickness. Curves a, b, c (green, purple, blue) represent the loading, mid-span and support locations. (1) Unidirectional (2) Quasi-isotropic (3) Cross-ply.

rollers, then the shear should vanish and the stress state would become of pure constant bending moment. In the practice, it takes about 1/6 of the length for the shear stress to drop to zero, both at the inner and outer noses, and the value that it attains in between is not constant but peaks within 1/12 of the length.

4. Conclusions

The main purpose of the paper was to investigate the possibility of using the static ILSS data obtained by testing simple unidirectional laminates to infer the properties of

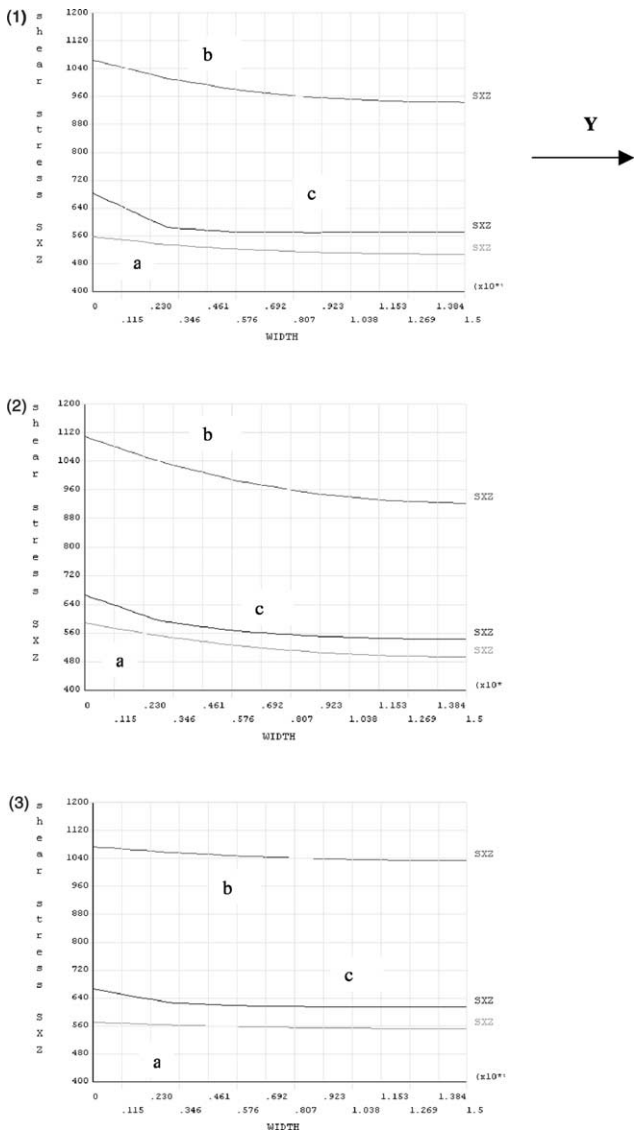

Fig. 8. 1/4 Model of ILS coupon: shear stress distribution across the width. Curves a, b, c (green, purple, blue) represent the loading, mid-span and support locations. (1) Unidirectional (2) Quasi-isotropic (3) Cross-ply.

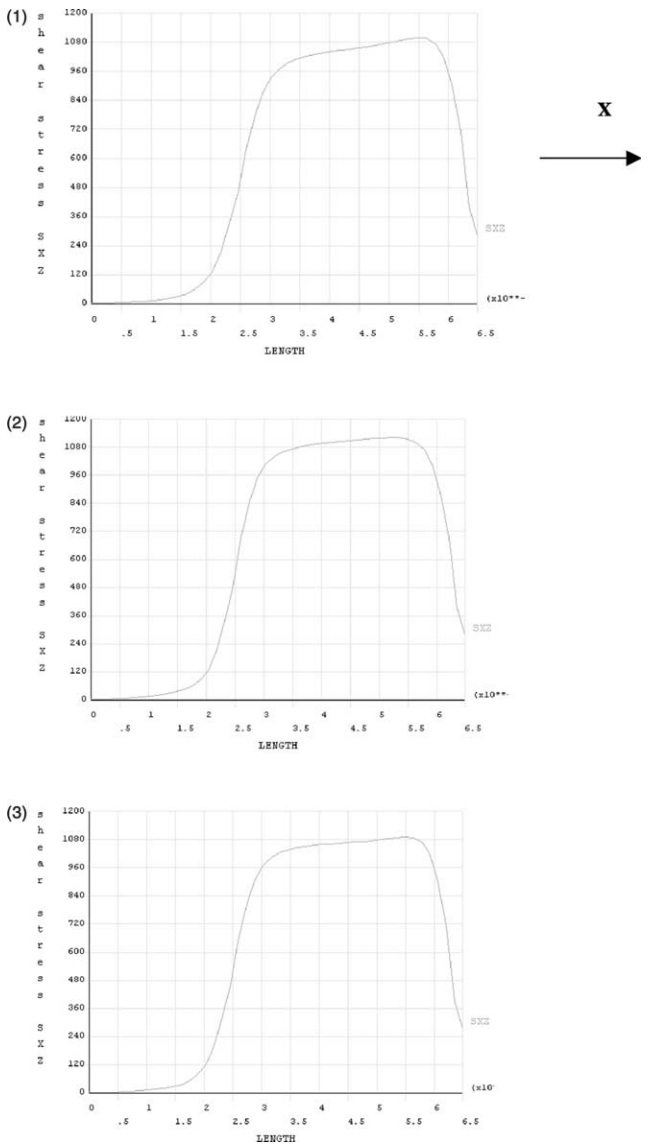

Fig. 9. 1/4 Model of ILS coupon: shear stress distribution along the length. (1) Unidirectional (2) Quasi-isotropic (3) Cross-ply.

more complex stacking sequences, in particular quasi-isotropic and cross-ply. The experimental and analytical data did confirm the validity of such investigation, see Table 5, therefore giving an answer to the question raised in Ref. [3] on the influence of the degree of orthotropy on the ILS strength. Finally, the matrix-dominated property of the ILSS was confirmed by its independence of fiber orientation and laminate lay-up.

Table 5
Shear stress predictions with average geometry and loading

Specimen	Unidirectional ksi (MPa)	Quasi-isotropic ksi (MPa)	Cross-ply ksi (MPa)
Beam theory max	10.86 (74.9)	10.19 (70.3)	11.02 (76.0)
Test data (average)	11.10 (76.57)	11.16 (76.93)	11.10 (76.52)
FEA (contour)	11.22 (77.37)	11.01 (75.94)	10.94 (75.44)
Kedward (peak width)	11.27 (77.7)	11.21 (77.3)	11.14 (76.8)

Furthermore, the shear stress distributions through the thickness and across the width reported in Refs. [3,4,9] for unidirectional laminates were confirmed for the other configurations with the aid of a three-dimensional finite element model, and the results obtained with the closed form solution and the model were in perfect agreement. From the detailed shear stress contour it was possible to discover the point of maximum stress in a region within one thickness away from the supporting roller for all three laminates. This is the suspected location of delamination origination, which leads to classical interlaminar failure, also defined as unstable fracture [10], and it confirms

previous in situ observation made by the authors and others.

Acknowledgements

Paolo would like to thank first and foremost Keith Kedward, co-author of the paper but in reality its real inspirer, as well as his mentor, guide and friend who introduced him to the world of composites. In addition, thanks are due to Yuqiao Zhu for helping with fundamental inputs on the FEA work. They also would like to acknowledge the work of their colleague and friend Attilio Masini, Automobili Lamborghini, who has successfully introduced aerospace grade carbon/epoxy prepreg materials in the high-end commercial vehicle production.

References

[1] ASTM standard D2344/ D2344M. Apparent interlaminar shear strength of unidirectional parallel fiber composites by short beam method; 2000.

[2] Adams D, Lewis E. Experimental study of three- and four-point shear test specimens, ASTM. ; 1995.

[3] Xie M, Adams D. Study of three- and four-point shear testing of unidirectional composite materials. Composites 1995;26:9.

[4] Kedward K. On the short beam test method. Fibre Sci Technol 1972; (5):85–95.

[5] Post D. Shear strains in a graphite/PEEK beam by Moiré interferometry with carrier fringes. SEM Fall Conference on Experimental Mechanics, Keystone, CO; 1986.

[6] ASTM standard D790. Flexural properties of unreinforced and reinforced plastics; 1999.

[7] Whitney JM, Browning CE. On short beam shear tests for composite materials. Exp Mech 1985;294–300.

[8] Whitney JM. Elasticity analysis of orthotropic beams under concentrated loads. Compos Sci Technol 1985;22:167–84.

[9] Wisnom MR. Modeling of stable and unstable fracture of short-beam shear specimens. Composites 1994;25:6.

[10] John NSt, Brown J. Flexural and interlaminar shear properties of glass-reinforced phenolic composites. Composites, Part A 1998; 29A.

[11] Sullivan JL, Van Oene H. An elasticity analysis for orthotropic beams subjected to concentrated loads. Compos Sci Technol 1986;27: 133–55.

[12] Sayers K. Interlaminar shear strength of a carbon fiber reinforced composite material under impact conditions. Compos Mater 1973; 7:129.